Tumor-derived osteopontin isoforms cooperate with TRP53 and CCL2 to promote lung metastasis.

Ioanna Giopanou[1,3], Ioannis Lilis[1], Vassilios Papaleonidopoulos[1], Theodora Agalioti[1], Nikolaos I. Kanellakis[1], Nikolitsa Spiropoulou[1], Magda Spella[1], and Georgios T. Stathopoulos[1,2,3].

[1] *Laboratory for Molecular Respiratory Carcinogenesis, Department of Physiology, Faculty of Medicine; University of Patras; Rio, Achaia, 26504; Greece.*

[2] *Comprehensive Pneumology Center (CPC) and Institute for Lung Biology and Disease (iLBD); University Hospital, Ludwig-Maximilians University and Helmholtz Zentrum München, Member of the German Center for Lung Research (DZL); Munich, Bavaria, 81377; Germany.*

[3] *Co-corresponding* authors.

Corresponding authors: Georgios T. Stathopoulos, MD PhD (gstathop@upatras.gr) and Ioanna Giopanou, PhD (giopanou@upatras.gr).

Running title: Osteopontin isoforms in lung metastasis

ABSTRACT

The lungs are ubiquitous receptacles of metastases originating from various bodily tumors. Although osteopontin (SPP1) has been associated with tumor dissemination, the role of its isoforms in lung-directed metastasis is incompletely understood. We employed syngeneic mouse models of spontaneous and induced lung-targeted metastasis in *C57BL/6* mice competent and deficient in both *Spp1* alleles. Tumor-derived osteopontin expression was modulated using either stable anti-*Spp1* RNA interference, or forced overexpression of intracellular and secreted *Spp1* isoforms. Identified osteopontin's downstream partners were validated using lung adenocarcinoma cells conditionally lacking the *Trp53* gene and *Ccr2*-deficient mice. We determined that host derived osteopontin was dispensable for pulmonary colonization by different tumor types. Oppositely, tumor originated intracellular osteopontin promoted tumor cell survival by preventing tumor-related protein 53-mediated apoptosis, while the secretory osteopontin functioned in a paracrine mode to accelerate lung metastasis by enhancing tumor-derived C-C-motif chemokine ligand 2 signaling to cognate host receptors. As new ways to target osteopontin signaling are becoming available, the cytokine may constitute an important therapeutic target against pulmonary involvement by cancers of other organs.

Keywords: C-C-motif chemokine ligand 2, inflammation and cancer, Secreted phosphoprotein 1, spontaneous lung metastasis, tumor-related protein 53.

INTRODUCTION

Pulmonary metastasis is frequent in patients suffering from various tumors, especially adenocarcinomas of the lungs, breast, and colon, and is a major cause of cancer-related death [1-3]. Systemic tumor dissemination involves complex interactions between tumor and host cells during the intravasation of tumor cells into blood and/or lymphatic vessels at the primary tumor site, their spread to target organs, and their survival and extravasation at distant sites [4]. These processes are dictated by genetic and epigenetic alterations of tumor cells that cross-talk to the host microenvironment to facilitate intercellular communication, immune evasion, and sustained proliferation, and such traits of metastasis present lucrative targets for therapy [5].

Osteopontin (also known as secreted phosphoprotein 1, SPP1), an adhesive glycophosphoprotein widely expressed in tissues, body fluids, and cells under normal conditions, regulates physiologic processes such as development, differentiation, inflammation, and wound healing [6-9]. In addition, SPP1 is highly expressed in the microenvironment of various tumors, both by malignant and host cells [10-12]. Osteopontin has been linked with enhanced tumor progression and metastasis by modulating cell-cell interactions, by activating signal transduction pathways, by altering gene expression, and by promoting tumor cell survival [13-20]. Interestingly, the diverse effects of SPP1 vary between cell types and target organs of metastasis, depending on which signaling pathways are activated and which isoforms of the protein are expressed [16, 21, 22]. Despite significant efforts, a comprehensive understanding of the functions of cancer- and host-originated SPP1 isoforms during pulmonary metastasis is elusive.

In this study, we asked whether host- or tumor-derived, intracellular (iSPP1) or secreted (sSPP1) SPP1 isoforms promote pulmonary dissemination of different tumor types and searched for the specific mechanisms of their involvement in this phenomenon. To address these questions, we combined several novel approaches: i) syngeneic mouse models of both spontaneous and induced pulmonary metastasis on a background of full immunocompetence; ii) tumor cell lines of different tissues of origin featuring different SPP1expression patterns; iii) SPP1 silencing; iv) engineering and overexpression of eukaryotic vectors encoding different SPP1 isoforms; v) conditionally *Trp53*-deleted primary lung adenocarcinoma cells; and vi) *Ccr2* gene-deficient mice. We identified distinct roles for intracellular and secreted SPP1 isoforms expressed by tumor cells during pulmonary metastatic colonization. The former prolonged tumor cell survival in a cell-autonomous fashion and the latter enhanced metastasis *in vivo* via paracrine signaling to host cells.

RESULTS

Characterization of mouse osteopontin transcript protein products.

Since there is no definite way in literature to distinguish between the protein products of the two main murine *Spp1* transcripts, *Spp1is2* and *Spp1is4*, due to their similar molecular weight [23], we initially aimed to characterize and correlate the main murine *Spp1* transcripts with their corresponding proteins. For this, we transfected HEK293T cells with bicistronic vectors encoding murine *Spp1* isoforms in-frame with GFP or GFP alone. The generation of these vectors is described in detail in the Appendix PDF. Transfection of HEK293T cells with *Spp1is2.GFP* resulted in expression of a single protein of an apparent mass of 68 KDa. Transfection of HEK293T cells with *Spp1is4.GFP* resulted in both the above-mentioned 68 KDa band and an additional

band that consistently appeared at 50 KDa (Fig. 1A). These results positioned the molecular mass of the *Spp1is2* and *Spp1is4* transcripts' protein products at approximately 41 KDa, and at 41 and 23 KDa, respectively, since GFP separates at 27 KDa (Fig. 1A). The selective appearance of the 23 KDa protein upon overexpression of *Spp1is4* was deemed to result from cleavage specific only for this transcript's protein product; the resulting 23 KDa fragment, a product of post-translational modifications, has been reported to be the secreted protein product [24]. From these studies and the literature we concluded that translation of *Spp1is2* results in a 41 KDa cytoplasmic protein, hereafter called intracellular SPP1 (iSPP1), while translation of *Spp1is4* in both an unprocessed iSPP1 isoform and a processed, secretory SPP1 isoform (sSPP1).

Host osteopontin expression and its impact on lung metastasis.

We next characterized osteopontin expression in naïve mouse lungs and blood, the anatomic compartments where lung metastasis is initiated. Osteopontin immunoreactivity was evident in non-ciliated airway epithelial (Clara or club) cells, as well as alveolar macrophages, but not in ciliated airway and alveolar epithelial, mesothelial, and pulmonary endothelial cells (Fig. 1B and S1A, S1B). Osteopontin protein was also present in the bloodstream of *Spp1* gene-competent ($Spp1^{+/+}$) and of single-allele *Spp1* gene-deficient ($Spp1^{+/-}$), but not of homozygote *Spp1* knock-out ($Spp1^{-/-}$) *C57BL/6* mice (Fig. S1C; [9]. Immunoblotting of whole lung protein extracts from $Spp1^{+/+}$ and $Spp1^{-/-}$ mice and from HEK293T human embryonic kidney cells, known to produce iSPP1 and sSPP1 [25], revealed predominant expression of processed sSPP1 in the lungs (Fig. S1D). Unexpectedly, host-derived osteopontin did not impact spontaneous and forced pulmonary metastasis. To test this, $Spp1^{+/+}$

and *Spp1*$^{-/-}$ mice received three different origin cancer cell lines derived from *C57BL/6* mice: B16F10 skin melanoma, Lewis lung carcinoma (LLC), and MC38 colon adenocarcinoma. Tumor cell injections were done both subcutaneously (s.c.), and intravenously (i.v.) in separate cohorts of mice. As shown in Fig. 1C, *Spp1*$^{+/+}$ and *Spp1*$^{-/-}$ mice with s.c. LLC or MC38 cells displayed similar flank tumor growth rates, while *Spp1*$^{-/-}$ mice with s.c. B16F10 cells exhibited decreased primary tumor growth compared with *Spp1*$^{+/+}$ mice. Importantly, only LLC cells could spontaneously metastasize to the lungs, with *Spp1*$^{+/+}$ *and Spp1*$^{-/-}$ mice displaying equal number and size of lung lesions, as determined by both gross lung tumor counting and morphometry of randomly sampled lung sections [26, 27]. Similar results were obtained after i.v. delivery of tumor cells. All cancer cell lines colonized the lungs upon tail vein injection, with *Spp1*$^{+/+}$ *and Spp1*$^{-/-}$ mice developing similar number and size of lung lesions (Fig. 1D and S1E). These results suggested that host-originated osteopontin is not cardinal for pulmonary metastasis.

Differential SPP1 isoform expression by tumor cells.

We next investigated tumor cells as a source of osteopontin. For this, B16F10, LLC, and MC38 cells were assessed for expression of osteopontin transcripts and protein by reverse transcriptase (RT)-PCR, immunoblotting, immunocytochemistry, and ELISA (Fig. 2A-2D). In parallel to parental cells, daughter cells stably overexpressing eukaryotic expression vectors encoding murine *Spp1is2* and *Spp1is4*, as well as random control (sh*C*) or anti-*Spp1* (sh*Spp1*) shRNA were generated. We determined that B16F10 cells express minimal amounts of both osteopontin transcripts and their corresponding proteins, that LLC cells express similar amounts of both transcripts,

while MC38 cells predominantly express *Spp1is4* and processed sSPP1. In addition, we validated our daughter cell lines with modulated osteopontin isoform expression.

iSPP1 as a cell-autonomous tumor cell survival signal that requires wild-type TRP53. We next determined the proliferation and apoptosis rates of our parental and *Spp1*-modulated cell lines *in vitro* using MTT assay, labeling with annexin V and 7-aminoactinomycin D (7AAD), as well as immunostaining for caspases 3 and 8 (Fig. 2E-2G and S2). We observed that overexpression of *Spp1is2* in B16F10 cells that are osteopontin-deficient resulted in enhanced cell proliferation and diminished apoptotic indices, while overexpression of *Spp1is4* in these cells did not impact cell proliferation. Moreover, silencing of *Spp1* in LLC cells (competent in both osteopontin isoforms) significantly inhibited cell proliferation, augmented apoptosis, and induced caspases 3 and 8, while the same intervention in MC38 cells (predominantly competent in sSPP1) had no effect on these parameters. These results indicated that iSPP1 (encoded by *Spp1is2*) promotes tumor cell survival in a cell-autonomous fashion. We next subjected parental and *Spp1*-silenced LLC and MC38 cells to analysis of global gene expression. Interestingly, *Spp1* silencing affected chemokine and cytokine signaling pathways in both cell types, but selectively perturbed the tumor-related protein 53 (TRP53) signaling pathway in LLC cells (Fig. S3A). In specific, *Spp1* silencing in LLC cells induced key TRP53 pathway components that lead to activation of effector caspases 3 and 8, while the same intervention in MC38 cells suppressed several TRP53 pathway components (Fig. S3B). TRP53 immunostaining revealed that LLC cells showed minimal TRP53 immunoreactivity that was enhanced upon *Spp1* silencing, whereas MC38 cells displayed high TRP53 expression that was not affected by *Spp1* shRNA (Fig. S4A). This pattern indicated a *Trp53* mutation in MC38 cells that results in increased

stability of non-functional TRP53 protein. Indeed, Sanger sequencing and immunofluorescence confirmed a heterozygous *Trp53*^{R178P} point mutation and ubiquitous nuclear non-labile TRP53 protein in these cells (Fig. S4B and S4C). These findings suggested that cell-autonomous pro-survival effects of osteopontin in tumor cells may be mediated by wild-type TRP53. To definitely test this in an isogenic cellular system, we derived a lung adenocarcinoma cell line from conditionally *Trp53*-deleted mice [*Trp53*$^{f/f}$; [28]]. For this, *Trp53*$^{f/f}$ mice (*C57BL/6* strain) received ten weekly intraperitoneal injections of the lung carcinogen urethane (1 g/Kg), as described elsewhere [29, 30], and were sacrificed after 10 months, followed by long-term lung tumor culture *in vitro*. The resulting cell line (*C57BL/6* Urethane-induced Lung Adenocarcinoma, CULA) was tumorigenic and spontaneously metastatic to the lungs when implanted s.c. in *C57BL/6* mice, and was efficiently recombined *in vitro* using a *Cre* recombinase plasmid [31], yielding isogenic tumor cells with or without functional *Trp53* alleles (Fig. 3A-3J). Using this system combined with *Spp1* shRNA, we determined that osteopontin silencing decreased proliferation and increased apoptosis of parental CULA cells with functional *Trp53* alleles, while this effect was lost upon *Trp53* deletion (Fig. 3K-3M), confirming a role for wild-type TRP53 in the cell-autonomous pro-survival effects of iSPP1.

Tumor-derived sSPP1 as a driver of lung metastasis that signals via CCL2 to host cells.

We next injected B16F10, LLC, and MC38 parental and modulated daughter cells s.c. or i.v. to *C57BL/6* mice and assessed their potential for lung metastasis. Overexpression of osteopontin isoforms in B16F10 cells and silencing of osteopontin in MC38 cells had no apparent effects on flank tumor growth, but silencing of SPP1

in LLC cells resulted in decreased tumor growth, reduced spontaneous lung metastases, and prolonged survival of mice with s.c. tumors (Fig. 4). Moreover, overexpression of both osteopontin isoforms in naturally osteopontin-deficient B16F10 cells enhanced i.v. lung metastasis, with *Spp1is4* (encoding sSPP1) exhibiting greater effects (Fig. 5A). In addition, *Spp1* silencing abrogated lung metastasis and prolonged the survival of *C57BL/6* mice after i.v. delivery of LLC or MC38 cells (Fig. 5A-5C). These results indicated marked pro-metastatic effects of tumor-derived sSPP1. We next analyzed microarrays from parental and *Spp1*-silenced LLC and MC38 cells for individual transcripts and identified *Ccl7* and *Ccl2* (encoding C-C-motif chemokine ligands 2 and 7, CCL2 and CCL7, respectively) as the top mRNAs down-regulated in both cells by sh*Spp1* (Fig. 6A and S5A; Tables S3 and S4). This was confirmed by qPCR, which showed that: i) tumor cell *Ccl2* expression predominated over that of *Ccl7*; ii) *Spp1is4* overexpression in B16F10 cells augmented *Ccl2* and *Ccl7* expression; and that iii) sh*Spp1* significantly inhibited *Ccl2*, but not *Ccl7*, expression in LLC and MC38 cells (Fig. 6B). These data were confirmed at protein level (Fig. S5B), identified CCL2 as a possible accomplice of sSPP1, and prompted us to evaluate the expression of *Ccl2* and its receptor *Ccr2* in the hosts and tumor cells of our models. In addition to bone marrow and liver, the lungs expressed significant levels of *Ccr2*, while *Ccl2* was exclusively expressed by LLC and MC38 cells (Fig. 6C). To test whether CCL2 signaling by tumor cells to host CCR2 receptors mediates the pro-metastatic effects of sSPP1, we injected MC38 cells (predominantly expressing sSPP1), *Spp1*-silenced MC38 cells, B16F10 cells (iSPP1 and sSPP1-deficient), and B16F10 cells overexpressing either *Spp1is2* or *Spp1is4* into the bloodstream of *Ccr2*-deficient and control mice bred on a pure *C57BL/6* strain [32]. These experiments showed that host CCR2-competence is

important during lung metastasis of sSPP1-competent cells but dispensable for pulmonary colonization by sSPP1-deficient tumor cells, and confirmed that tumor-derived sSPP1 functions via signaling to host CCR2 receptors (Fig. 6D-6E and S6).

DISCUSSION

We studied the role of osteopontin isoforms in lung metastasis by mapping their expression by tumor and host cells and by using hosts and tumor cells that feature loss or gain of their expression. Syngeneic, immunocompetent mouse models of pulmonary metastasis of both subcutaneous and intravenous cancer cells were employed to capture intact tumor-host interactions. We describe the distinct functions of tumor-derived osteopontin isoforms, including the *in vitro* pro-survival effects of iSPP1 and the *in vivo* pro-metastatic effects of sSPP1, and pin wild-type TRP53 and CCL2 as their respective signaling partners. Our results can be translated to strategies of osteopontin targeting against metastasis and are important on several counts.

First, tumor-derived osteopontin is corroborated as a culprit of lung metastasis of various tumor types, in line with published work [15, 33]. Both in our and other studies, osteopontin effects were delivered during late-stage metastasis, since similar results were obtained from s.c. and i.v. models [15, 33]. Hence the cytokine is likely dispensable for tumor dissemination from the primary site, but is required for circulating tumor cell engraftment in the lungs. Since circulating tumor cells are ubiquitous in cancer patients with minimal disease and most cancer patients will already have metastasis at the time of diagnosis [4, 5], mediators of end-organ colonization such as osteopontin are marked targets for therapy. Thus our findings bear potential clinical implications, as several approaches to inhibit osteopontin

signaling are in development [34, 35]. Our negative results from osteopontin-deficient mice are different from findings from breast cancer and malignant pleural effusion (MPE) models where host osteopontin was important [15, 16]. However, the different results can be reconciled and convey mechanistic implications: the different models employed in these studies feature divergent anatomic and cellular compartmentalization of osteopontin expression and different osteopontin expression patterns by tumor cells [36]. Since osteopontin impacts late-stage metastasis, the local levels of tumor- and host-delivered osteopontin in the incipient metastatic niche are likely critical. Interestingly, *Balb/c* mice feature high serum osteopontin levels compared with *C57BL/6* mice [37], and 4T1 cells secrete less osteopontin compared with LLC and MC38 cells (1 versus 20-40 μg/ml/10^6 cells/24 hours, respectively), likely rendering host osteopontin important in 4T1 cell metastasis [15], but not in our hands. Similarly, we measured elevated levels of host osteopontin in MPE [16] as compared with the bloodstream in our study (300 versus 70 ng/ml, respectively), making host osteopontin important in MPE [16], but not in the work presented here. In our hands, the pulmonary endothelium did not express osteopontin and the bulk of local osteopontin was delivered by metastatic tumor cells, rendering tumor-expressed osteopontin pivotal for lung colonization. These observations likely explain the role of host osteopontin in the support of tumor growth when B16F10 cells were delivered s.c., since these cells do not express the cytokine and likely depend on host-derived osteopontin.

Second, we define the distinct functions of osteopontin isoforms during pulmonary metastasis. As previously reported on the distinct adhesive properties of murine osteopontin that result from cell specific post-translational modifications [38], we show that iSPP1 and sSPP1 are differentially expressed by tumor cells, with the former

preventing TRP53 stabilization and apoptosis, and the latter signaling to host CCR2 receptors via CCL2 to promote lung homing. Our results corroborate previous work on the inhibition of apoptosis [39] and the involvement of TRP53 in iSPP1-dependent anti-apoptotic signaling [40] and show for the first time that the pro-survival effects of osteopontin in cancer cells are conditional on wild-type *TRP53*. Our findings imply that targeting of human iSPP1 in clinical trials may be selectively effective against *TRP53* wild-type tumors and provide a rationale for stratification of patients by *TRP53* status. This notion is of special importance for neoplasms where osteopontin biology is cardinal and *TRP53* mutations frequent, such as malignant pleural mesothelioma [16, 41-43].

Third, sSPP1 is identified as the key osteopontin isoform that promotes lung metastasis across tumor types. To this end, overexpression of the corresponding transcript *Spp1is4* exerted a far stronger pro-metastatic impact on naturally osteopontin-deficient B16F10 cells, compared with the transcript *Spp1is2* that corresponds to iSPP1. These data explain the results of previous studies implicating osteopontin in tumor cells, as well as its receptor CD44 on host cells, in metastasis to other sites [15, 44, 45]. Furthermore, our results bear clinical implications for selective osteopontin isoform targeting, since selective sSPP1 inhibition can be accomplished using protein and RNA-based methods [35].

Furthermore, sSPP1 is identified to exert its pro-metastatic function by regulating tumor-to-host CCL2/CCR2 signaling. Our data reconcile the results of previous studies on breast cancer [15, 46] and help explain the mononuclear chemoattractant function of tumor-originated osteopontin observed by others. For the first time, murine osteopontin functions during *in vivo* metastasis are linked with CCL2

signaling, a known druggable trait of thoracic tumor dissemination [47-50]. CCL2 can, in turn, enhance osteopontin signaling, since it augments the expression of the osteopontin receptor a_vb_3 integrin [51, 52]. Both molecules activate pathways such as FAK/Akt, MAPK, JAK2-Stat5, p38MAPK, and NF-κB in endothelial cells, thereby promoting adhesion, extravasation, and immune evasion of circulating tumor cells [18-21]. Importantly, CCL2 provides a direct explanation for the pro-metastatic effects of sSPP1, since CCR2 signaling in pulmonary endothelial cells directly promotes circulating tumor cell extravasation in the lungs[52]. In addition, the findings bear implications for future targeting of sSPP1 against metastasis in terms of combined sSPP1/CCL2 inhibition, pre-treatment screens for sSPP1/CCL2 expression, and CCL2 blockade against sSPP1-expressing tumors [48, 50, 53].

In conclusion, we comprehensively mapped the expression patterns, the distinct functions, and the key downstream signaling partners of intracellular and secretory osteopontin isoforms during pulmonary metastasis. We provide proof-of-concept evidence that can be useful for the design of future preclinical and clinical studies aimed at targeting this metastatic trait.

MATERIALS AND METHODS

Detailed Supplementary Materials and Methods can be found with this article online.

Mice

C57BL/6 (#000664), *B6.129S6-Spp1*$^{tm1Blh/J}$ (#004936), *B6.129P2-Trp53*$^{tm1Brn/J}$ (#008462), and *B6.129S4-Ccr2*$^{tm1Ifc/J}$ (#004999) mice obtained from Jackson Laboratories (Bar Harbor, ME) were bred in the University of Patras Center for Animal Models of Disease. Experiments were designed and approved *a priori* by the local Veterinary Administration of the Prefecture of Western Greece (approvals # 3741/16.11.2010, 60291/3035/19.03.2012, and 118018/578/30.04.2014), and were conducted according to Directive 2010/63/EU. Male and female experimental mice and littermate controls were sex-, weight (20-25 g)-, and age (6-12 week)-matched (for *n* see Table S4).

Cells and constructs

LLC and B16F10 cells were from the National Cancer Institute Tumor Repository (Frederick, MD); MC38 cells were a gift from Dr. Timothy S. Blackwell [Vanderbilt University, Nashville, TN; [53]; and HEK293T cells were from the American Type Culture Collection (Manassas, VA). Cell lines were cultured in DMEM and tested biannually for identity and stability by short tandem repeats, Sanger sequencing for driver mutations, and microarray. Anti-*Spp1* shRNA (16) and SPP1 isoform constructs are described in the online SI.

Metastasis models

For development of flank tumors and spontaneous lung metastases, 10^6 LLC, 10^6 MC38, or 0.25 x 10^6 B16F10 cells were injected s.c. For induction of forced lung metastases, 0.25 x 10^6 LLC, 0.25 x 10^6 MC38, or 0.15 x 10^6 B16F10 cells were injected into the tail vein. These numbers were tittered in preliminary experiments to yield 100% tumor take. Mice were sacrificed 30 days after s.c. or 14 days after i.v. tumor cells for metastasis analyses, or when moribund for survival analyses. Lungs were fixed in 10% neutral buffered formalin overnight and the number of lung metastasis was evaluated by two blinded investigators (I. G. and G. T. S.) and averaged. Lung volume was measured by saline immersion, and lungs were embedded in paraffin, randomly sampled by cutting 4µm-thick lung sections (*n* = 10/lung), mounted on glass slides, and stained with H&E. Lung tumor burden was determined by point counting of the ratio of the area occupied by metastases versus the lung area and by extrapolating the average ratio per mouse to total lung volume, as described elsewhere [27].

Primary mouse lung adenocarcinoma cells

Trp53$^{f/f}$ mice (*C57BL/6* strain) received ten consecutive weekly intraperitoneal injections of the pulmonary carcinogen urethane (1g/kg) starting at six weeks of age and were sacrificed ten months later. Select lung tumors (*n* = 10) were isolated under sterile conditions for culture and the remaining lungs were fixed for histology. Lung tumor cells were cultured for more than 100 passages over two years to successfully yield one tumor cell line (CULA).

Statistics

Data are expressed as mean ± SD. Differences in means between two or multiple groups were examined by two-tailed Student's t-test or one-way ANOVA with Bonferoni post-tests, as appropriate, since data were distributed normally. Two-way ANOVA with Bonferoni post-tests was employed for analyses of cell and tumor growth. Survival proportions were examined by Kaplan-Meier analysis and log-rank test. All *P* values are two-tailed and were considered significant when < 0.05. All statistics and plots were done using Prism v5.0 (GraphPad, La Jolla, CA).

ACKNOWLEDGEMENTS

This work was supported by European Research Council 2010 Starting Independent Investigator and 2015 Proof of Concept Grants (260524 and 679345, respectively, to G.T.S.). The authors thank the University of Patras Center for Animal Models of Disease. The authors report no conflict of interest.

AUTHOR'S CONTRIBUTIONS

I. G. performed most of the experiments; I. L., V. P., T. A., N.S., and M.S performed several *in vitro* assays and provided critical intellectual input; N. I. K. analyzed the microarray data and performed Quantitative Real-time PCR; I. G. and G. T. S. designed the experiments, analyzed the data, and wrote the paper; G. T. S. conceived the idea and supervised the study, and is the guarantor of the study's integrity. All authors reviewed and concur with the submitted manuscript.

CONFLICT OF INTEREST

The authors report no conflict of interest.

ACCESSION NUMBERS

All plasmids were deposited with Addgene and their ID's are given in the text. Microarray data were deposited at GEO database (http://www.ncbi.nlm.nih.gov/geo/; Accession ID: GSE79831.

SUPPLEMENTARY MATERIAL

Supplementary Materials and Methods and can be found with this article online.

REFERENCES

1. Hess KR, Varadhachary GR, Taylor SH, Wei W, Raber MN, Lenzi R, et al. Metastatic patterns in adenocarcinoma. Cancer 2006; 106:1624-33.
2. Disibio G, French SW. Metastatic patterns of cancers: results from a large autopsy study. Arch Pathol Lab Med 2008; 132:931-9.
3. Sethi N, Kang Y. Unravelling the complexity of metastasis - molecular understanding and targeted therapies. Nat Rev Cancer 2011; 11:735-48.
4. Nguyen DX, Bos PD, Massague J. Metastasis: from dissemination to organ-specific colonization. Nat Rev Cancer 2009; 9:274-84.
5. Vanharanta S, Massague J. Origins of metastatic traits. Cancer Cell 2013; 24:410-21.
6. Ashkar S, Weber GF, Panoutsakopoulou V, Sanchirico ME, Jansson M, Zawaideh S, et al. Eta-1 (osteopontin): an early component of type-1 (cell-mediated) immunity. Science 2000; 287:860-4.
7. Zheng W, Li R, Pan H, He D, Xu R, Guo TB, et al. Role of osteopontin in induction of monocyte chemoattractant protein 1 and macrophage inflammatory protein 1beta through the NF-kappaB and MAPK pathways in rheumatoid arthritis. Arthritis Rheum 2009; 60:1957-65.
8. Li G, Oparil S, Kelpke SS, Chen YF, Thompson JA. Fibroblast growth factor receptor-1 signaling induces osteopontin expression and vascular smooth muscle cell-dependent adventitial fibroblast migration in vitro. Circulation 2002; 106:854-9.
9. Liaw L, Birk DE, Ballas CB, Whitsitt JS, Davidson JM, Hogan BL. Altered wound healing in mice lacking a functional osteopontin gene (spp1). J Clin Invest 1998; 101:1468-78.
10. Bramwell VH, Tuck AB, Chapman JA, Anborgh PH, Postenka CO, Al-Katib W, et al. Assessment of osteopontin in early breast cancer: correlative study in a randomised clinical trial. Breast Cancer Res 2014; 16:R8.
11. Fedarko NS, Jain A, Karadag A, Van Eman MR, Fisher LW. Elevated serum bone sialoprotein and osteopontin in colon, breast, prostate, and lung cancer. Clin Cancer Res 2001; 7:4060-6.
12. Agrawal D, Chen T, Irby R, Quackenbush J, Chambers AF, Szabo M, et al. Osteopontin identified as lead marker of colon cancer progression, using pooled sample expression profiling. J Natl Cancer Inst 2002; 94:513-21.
13. Khodavirdi AC, Song Z, Yang S, Zhong C, Wang S, Wu H, et al. Increased expression of osteopontin contributes to the progression of prostate cancer. Cancer Res 2006; 66:883-8.
14. Yin M, Soikkeli J, Jahkola T, Virolainen S, Saksela O, Holtta E. Osteopontin promotes the invasive growth of melanoma cells by activating integrin alphavbeta3 and down-regulating tetraspanin CD9. Am J Pathol 2014; 184:842-58.
15. Sangaletti S, Tripodo C, Sandri S, Torselli I, Vitali C, Ratti C, et al. Osteopontin shapes immunosuppression in the metastatic niche. Cancer Res 2014; 74:4706-19.
16. Psallidas I, Stathopoulos GT, Maniatis NA, Magkouta S, Moschos C, Karabela SP, et al. Secreted phosphoprotein-1 directly provokes vascular leakage to foster malignant pleural effusion. Oncogene 2013; 32:528-35.
17. Bellahcene A, Castronovo V, Ogbureke KU, Fisher LW, Fedarko NS. Small integrin-binding ligand N-linked glycoproteins (SIBLINGs): multifunctional proteins in cancer. Nat Rev Cancer 2008; 8:212-26.

18. Lin YH, Yang-Yen HF. The osteopontin-CD44 survival signal involves activation of the phosphatidylinositol 3-kinase/Akt signaling pathway. J Biol Chem 2001; 276:46024-30.
19. Philip S, Bulbule A, Kundu GC. Osteopontin stimulates tumor growth and activation of promatrix metalloproteinase-2 through nuclear factor-kappa B-mediated induction of membrane type 1 matrix metalloproteinase in murine melanoma cells. J Biol Chem 2001; 276:44926-35.
20. Das R, Mahabeleshwar GH, Kundu GC. Osteopontin induces AP-1-mediated secretion of urokinase-type plasminogen activator through c-Src-dependent epidermal growth factor receptor transactivation in breast cancer cells. J Biol Chem 2004; 279:11051-64.
21. Crawford HC, Matrisian LM, Liaw L. Distinct roles of osteopontin in host defense activity and tumor survival during squamous cell carcinoma progression in vivo. Cancer Res 1998; 58:5206-15.
22. Bourassa B, Monaghan S, Rittling SR. Impaired anti-tumor cytotoxicity of macrophages from osteopontin-deficient mice. Cell Immunol 2004; 227:1-11.
23. Shinohara ML, Kim HJ, Kim JH, Garcia VA, Cantor H. Alternative translation of osteopontin generates intracellular and secreted isoforms that mediate distinct biological activities in dendritic cells. Proc Natl Acad Sci U S A 2008; 105:7235-9.
24. Sodek J, Ganss B, McKee MD. Osteopontin. Crit Rev Oral Biol Med 2000; 11:279-303.
25. Mirza M, Shaughnessy E, Hurley JK, Vanpatten KA, Pestano GA, He B, et al. Osteopontin-c is a selective marker of breast cancer. Int J Cancer 2008; 122:889-97.
26. Zaynagetdinov R, Sherrill TP, Gleaves LA, McLoed AG, Saxon JA, Habermann AC, et al. Interleukin-5 facilitates lung metastasis by modulating the immune microenvironment. Cancer Res 2015; 75:1624-34.
27. Hsia CC, Hyde DM, Ochs M, Weibel ER. An official research policy statement of the American Thoracic Society/European Respiratory Society: standards for quantitative assessment of lung structure. Am J Respir Crit Care Med 2010; 181:394-418.
28. Meylan E, Dooley AL, Feldser DM, Shen L, Turk E, Ouyang C, et al. Requirement for NF-kappaB signalling in a mouse model of lung adenocarcinoma. Nature 2009; 462:104-7.
29. Stathopoulos GT, Sherrill TP, Cheng DS, Scoggins RM, Han W, Polosukhin VV, et al. Epithelial NF-kappaB activation promotes urethane-induced lung carcinogenesis. Proc Natl Acad Sci U S A 2007; 104:18514-9.
30. Doris K, Karabela SP, Kairi CA, Simoes DC, Roussos C, Zakynthinos SG, et al. Allergic inflammation does not impact chemical-induced carcinogenesis in the lungs of mice. Respir Res 2010; 11:118.
31. Tashiro F, Niwa H, Miyazaki J. Constructing adenoviral vectors by using the circular form of the adenoviral genome cloned in a cosmid and the Cre-loxP recombination system. Hum Gene Ther 1999; 10:1845-52.
32. Boring L, Gosling J, Chensue SW, Kunkel SL, Farese RV, Jr., Broxmeyer HE, et al. Impaired monocyte migration and reduced type 1 (Th1) cytokine responses in C-C chemokine receptor 2 knockout mice. J Clin Invest 1997; 100:2552-61.
33. Kumar V, Behera R, Lohite K, Karnik S, Kundu GC. p38 kinase is crucial for osteopontin-induced furin expression that supports cervical cancer progression. Cancer Res 2010; 70:10381-91.

34. Mason CK, McFarlane S, Johnston PG, Crowe P, Erwin PJ, Domostoj MM, et al. Agelastatin A: a novel inhibitor of osteopontin-mediated adhesion, invasion, and colony formation. Mol Cancer Ther 2008; 7:548-58.
35. Bandopadhyay M, Bulbule A, Butti R, Chakraborty G, Ghorpade P, Ghosh P, et al. Osteopontin as a therapeutic target for cancer. Expert Opin Ther Targets 2014; 18:883-95.
36. Kazanecki CC, Uzwiak DJ, Denhardt DT. Control of osteopontin signaling and function by post-translational phosphorylation and protein folding. J Cell Biochem 2007; 102:912-24.
37. Schoensiegel F, Bekeredjian R, Schrewe A, Weichenhan D, Frey N, Katus HA, et al. Atrial natriuretic peptide and osteopontin are useful markers of cardiac disorders in mice. Comp Med 2007; 57:546-53.
38. Christensen B, Kazanecki CC, Petersen TE, Rittling SR, Denhardt DT, Sorensen ES. Cell type-specific post-translational modifications of mouse osteopontin are associated with different adhesive properties. J Biol Chem 2007; 282:19463-72.
39. Courter D, Cao H, Kwok S, Kong C, Banh A, Kuo P, et al. The RGD domain of human osteopontin promotes tumor growth and metastasis through activation of survival pathways. PLoS One 2010; 5:e9633.
40. Pass HI, Lott D, Lonardo F, Harbut M, Liu Z, Tang N, et al. Asbestos exposure, pleural mesothelioma, and serum osteopontin levels. N Engl J Med 2005; 353:1564-73.
41. Bueno R, Stawiski EW, Goldstein LD, Durinck S, De Rienzo A, Modrusan Z, et al. Comprehensive genomic analysis of malignant pleural mesothelioma identifies recurrent mutations, gene fusions and splicing alterations. Nat Genet 2016; 48:407-16.
42. Testa JR, Cheung M, Pei J, Below JE, Tan Y, Sementino E, et al. Germline BAP1 mutations predispose to malignant mesothelioma. Nat Genet 2011; 43:1022-5.
43. Gunthert U, Hofmann M, Rudy W, Reber S, Zoller M, Haussmann I, et al. A new variant of glycoprotein CD44 confers metastatic potential to rat carcinoma cells. Cell 1991; 65:13-24.
44. Sun J, Feng A, Chen S, Zhang Y, Xie Q, Yang M, et al. Osteopontin splice variants expressed by breast tumors regulate monocyte activation via MCP-1 and TGF-beta1. Cell Mol Immunol 2013; 10:176-82.
45. Sun SJ, Wu CC, Sheu GT, Chang HY, Chen MY, Lin YY, et al. Integrin beta3 and CD44 levels determine the effects of the OPN-a splicing variant on lung cancer cell growth. Oncotarget 2016.
46. Marazioti A, Kairi CA, Spella M, Giannou AD, Magkouta S, Giopanou I, et al. Beneficial impact of CCL2 and CCL12 neutralization on experimental malignant pleural effusion. PLoS One 2013; 8:e71207.
47. Stathopoulos GT, Psallidas I, Moustaki A, Moschos C, Kollintza A, Karabela S, et al. A central role for tumor-derived monocyte chemoattractant protein-1 in malignant pleural effusion. J Natl Cancer Inst 2008; 100:1464-76.
48. Zhang J, Lu Y, Pienta KJ. Multiple roles of chemokine (C-C motif) ligand 2 in promoting prostate cancer growth. J Natl Cancer Inst 2010; 102:522-8.
49. Qian BZ, Li J, Zhang H, Kitamura T, Zhang J, Campion LR, et al. CCL2 recruits inflammatory monocytes to facilitate breast-tumour metastasis. Nature 2011; 475:222-5.

50. Lin TH, Liu HH, Tsai TH, Chen CC, Hsieh TF, Lee SS, et al. CCL2 increases alphavbeta3 integrin expression and subsequently promotes prostate cancer migration. Biochim Biophys Acta 2013; 1830:4917-27.
51. Liaw L, Skinner MP, Raines EW, Ross R, Cheresh DA, Schwartz SM, et al. The adhesive and migratory effects of osteopontin are mediated via distinct cell surface integrins. Role of alpha v beta 3 in smooth muscle cell migration to osteopontin in vitro. J Clin Invest 1995; 95:713-24.
52. Wolf MJ, Hoos A, Bauer J, Boettcher S, Knust M, Weber A, et al. Endothelial CCR2 signaling induced by colon carcinoma cells enables extravasation via the JAK2-Stat5 and p38MAPK pathway. Cancer Cell 2012; 22:91-105.
53. Stathopoulos GT, Sherrill TP, Karabela SP, Goleniewska K, Kalomenidis I, Roussos C, et al. Host-derived interleukin-5 promotes adenocarcinoma-induced malignant pleural effusion. Am J Respir Crit Care Med 2010; 182:1273-81.

FIGURE LEGENDS

Figure 1 - Characterization of osteopontin transcript protein products and impact of host-expressed SPP1 on lung metastasis. A. Immunoblots probed with anti-SPP1 and anti-GFP antibodies of whole cell protein extracts of HEK293T cells (293T) transfected with no vector or with bicistronic vectors encoding *Spp1is2* or *Spp1is4* in-frame with GFP or GFP alone. Note the correspondence of the *Spp1is2* transcript to the iSPP1.GFP fusion protein that runs at ~ 68 KDa and of the *Spp1is4* transcript to the sSPP1.GFP fusion protein that runs at ~ 50 KDa, the GFP protein at ~ 27 KDa, as well as the ~ 40 KDa band appearing only after *Spp1is4* transfection, which likely represents a proteolytic fragment of osteopontin. B. Representative images of immunostaining of the main cell types and anatomic compartments of the naïve *C57BL/6* mouse lung (n = 5) for endogenous SPP1 (brown), counterstained with hematoxylin (blue). C, D. Primary tumor growth rate and number and total volume of lung metastases of *Spp1*-competent ($Spp1^{+/+}$) and Spp1-deficient ($Spp1^{-/-}$) mice after (C) s.c. injection (n = 5-7/group) or (D) i.v injection (n = 6-15/group) of B16F10, LLC, or MC38 cells. Note that only mice that received s.c LLC cells developed spontaneous lung metastases. Data are expressed as mean ± SD. ns and *: P > 0.05 and P < 0.05, respectively, for comparison between $Spp1^{+/+}$ and $Spp1^{-/-}$ mice by two-way ANOVA with Bonferroni post-tests (dot plots) or unpaired Student's t-test (bar graphs).

Figure 2 - SPP1 isoform expression by *C57BL/6* tumor cell lines and their role in cancer cell survival. A-D. Parental B16F10, LLC, and MC38 cells, B16F10 cells stably expressing *Spp1is2* and *Spp1is4* constructs (p), and LLC and MC38 cells stably expressing anti-*Spp1* (sh*Spp1*) or random control (sh*C*) shRNA were

assessed for *Spp1* mRNA by RT-PCR of total cellular RNA (A),SPP1 protein by immunoblotting of whole cells extracts (B), ELISA of cellular supernatants (C) and SPP1 cellular immunostaining (D). Inlays: isotype controls. Note amplicons of *Spp1is2* and *Spp1is4* at 933 and 885 bp, respectively, and the corresponding electrophoretic bands of iSPP1 and sSPP1 at 41 and 23 KDa (A and B). Note also that sSPP1 displays an apparent molecular mass that is smaller than anticipated by *Spp1is4* sequence due to post-translational modification (cleavage) (B). Finally note that only sSPP1 was detected in media conditioned for 24 hours by 10^5 live cells (n = 5/group) (C). E-G. Parental and SPP1-modulated tumor cells described above were assessed for cellular proliferation by MTT reduction (E) and for apoptosis by flow cytometric determination of annexin V and 7AAD staining (F) and caspase 3 and 8 immunoreactivity by immunocytochemistry (G). Data are expressed as mean ± SD of one representative of three experiments performed both in the presence or absence of 10% FBS. ns, **, and ***: $P > 0.05$, $P < 0.01$, and $P < 0.001$, respectively, for the indicated comparisons by by two-way (dot plots) or one-way (bar graphs) ANOVA with Bonferroni post-tests.

Figure 3 - A murine lung adenocarcinoma cell line conditional for *Trp53* alleles reveals that Trp53 is required for the pro-survival effects of intracellular SPP1. A. Strategy for derivation of *C57BL/6* Urethane-induced Lung Adenocarcinoma cells (CULA) from mice carrying loxP sites on either side of both *Trp53* alleles (*Trp53*$^{f/f}$). Mice (*n* = 5) were initiated on ten weekly intraperitoneal urethane injections (1 gr/kg) six weeks after birth and were sacrificed ten months after the first injection. Lungs were harvested under sterile conditions, tumors (*n* = 10) were enucleated, minced and cultured separately. One clone was established after four weeks and was passaged more than 100 times over two years. B. Representative stereoscopic image of lungs from *Trp53*$^{f/f}$ *C57BL/6* mouse treated as described under (A) featuring lung tumors (arrows). C, D. Representative images of immunostaining of lung tissue from *Trp53*$^{f/f}$ *C57BL/6* mouse treated as described under (A) for PCNA, shows minimal nuclear immunoreactivity in airway epithelium (arrows in C) in contrast to the significant proportion of immunoreactive cells (arrows) in urethane-induced tumors (dashed outline in D). E. Phase contrast image of *Trp53*$^{f/f}$ CULA cells in culture at passage 40. Note the spindle-shaped tumor cells. F-I. *C57BL/6* mice (*n* = 9) received 0.5 x 10^6 *Trp53*$^{f/f}$ CULA cells s.c. and were sacrificed after eight weeks. Representative images of flank tumor [dashed outline; (F)], spontaneous lung metastases [arrows; (G)], lung section with lung metastases [(H); arrows], and of lung section with lung metastasis showing several mitoses per high-power field [arrows; (I)]. J. RT-PCR of *Trp53*$^{f/f}$ CULA cells stably expressing vectors encoding a random sequence (p*C*) or CRE recombinase (p*Cre*). Successful deletion of floxed *Trp53* alleles is confirmed by the 270 bp product. K. Immunoblots of whole cell protein extracts of *Trp53*$^{f/f}$ CULA cells stably expressing vectors encoding a random sequence (p*C*) or CRE recombinase (p*Cre*) and random control (sh*C*) or *Spp1*-

specific shRNA (sh*Spp1*) showing efficient combined modulation of both TRP53 and SPP1 protein expression in this system. L, M. CULA cells featuring conditional *Trp53* alleles (*Trp53f/f*) were stably transfected as described in (K) were assessed for cellular proliferation by MTT reduction (L) and for apoptosis by flow cytometric determination of annexin V and 7AAD staining (M). Data are expressed as mean ± SD (*n* = 5/data-point) of one representative of three experiments performed both in the presence or absence of 10% FBS. ns, *, **, and ***: $P > 0.05$, $P < 0.05$, $P < 0.01$, and $P < 0.001$, respectively, for the indicated comparisons by two-way (dot plots) or one-way (bar graphs) ANOVA with Bonferroni post-tests.

Figure 4 - Tumor-derived SPP1 in spontaneous lung metastasis. Primary tumor growth rate (A-C), survival (D), and number (E), total volume (F), and representative images (G) of lung metastases of *C57BL/6* mice (*n* = 6-16/group) after s.c. injection of parental and SPP1-modulated tumor cells described in Figure 2. Note that only mice that received LLC cells developed spontaneous lung metastases. Shown are mean ± SD (all graphs except D) or Kaplan-Meier survival estimates (D). ns and ***: $P > 0.05$ and $P < 0.001$, respectively, for the indicated comparisons by two-way ANOVA with Bonferroni post-tests (dot plots), unpaired Student's t-test (bar graphs), or log-rank test (D).

Figure 5 - Tumor-derived SPP1 in induced lung metastasis. A, B. Number and total volume of lung metastases (A) and survival (B) of *C57BL/6* mice (*n* = 5-24/group) after i.v. injection of parental and SPP1-modulated tumor cells described in Figure 2. C. Representative microscopic images of lung sections stained with hematoxylin and eosin and stereoscopic images of lungs. Shown are mean ± SD (A) or Kaplan-Meier survival estimates (B). ns, *, **, and ***: $P > 0.05$, $P < 0.05$, $P <$

0.01, and P < 0.001, respectively, for the indicated comparisons by one-way ANOVA with Bonferroni post-tests [(A), B16F10 cells], unpaired Student's t-test [(A), LLC and MC38 cells], or log-rank test (B).

Figure 6 - A requirement for CCL2 in the pro-metastatic effects of sSPP1. A. Schematic of differential global gene expression by microarray of LLC and MC38 cells stably expressing anti-*Spp1*-specific (sh*Spp1*) or random control (sh*C*) shRNA. Listed are the top-ten common SPP1-dependent transcripts by order of magnitude. B. qPCR of total cellular RNA of parental and SPP1-modulated tumor cells described in figure 2 for *Ccl2* and *Ccl7* relative to *Gusb* mRNA (*n* = 3/data-point). Shown is one representative of three experiments. C. qPCR of total cellular and tissue RNA of parental tumor cells used in this study and of common target organs of metastasis for *Ccl2* and *Ccr2* relative to *Gusb* mRNA (*n* = 5/group). D, E. Number of lung metastases of *C57BL/6* mice competent ($Ccr2^{+/+}$) or deficient ($Ccr2^{-/-}$) in both *Ccr2* alleles after i.v. injection of parental and SPP1-modulated MC38 (D) and B16F10 (E) cells described in Figure 2 (*n* = 4-9/group). Data are expressed as mean ± SD. ns, *, **, and ***: P > 0.05, P < 0.05, P < 0.01, and P < 0.001, respectively, for the indicated comparisons (or comparison to brain in C) by one-way ANOVA with Bonferroni post-tests (B-D) or unpaired Student's t-test (E).

Figure 1

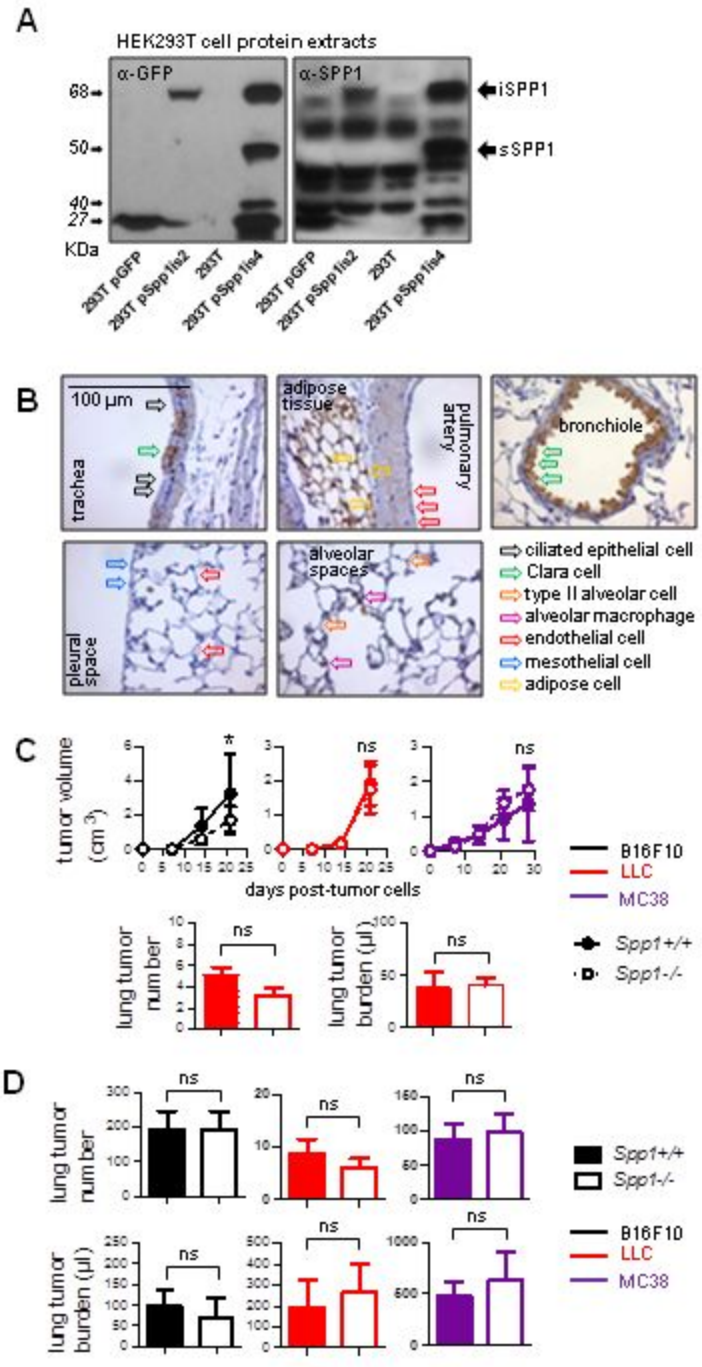
A
HEK293T cell protein extracts
α-GFP
α-SPP1
iSPP1
sSPP1
68
50
40
27
KDa
293T pGFP
293T pSpp1is2
293T
293T pSpp1is4
B
100 µm
trachea
adipose tissue
pulmonary artery
bronchiole
pleural space
alveolar spaces
ciliated epithelial cell
Clara cell
type II alveolar cell
alveolar macrophage
endothelial cell
mesothelial cell
adipose cell
C
tumor volume (cm3)
days post-tumor cells
B16F10
LLC
MC38
Spp1+/+
Spp1-/-
lung tumor number
lung tumor burden (µl)
ns
D
lung tumor number
lung tumor burden (µl)
Spp1+/+
Spp1-/-
B16F10
LLC
MC38

Figure 2

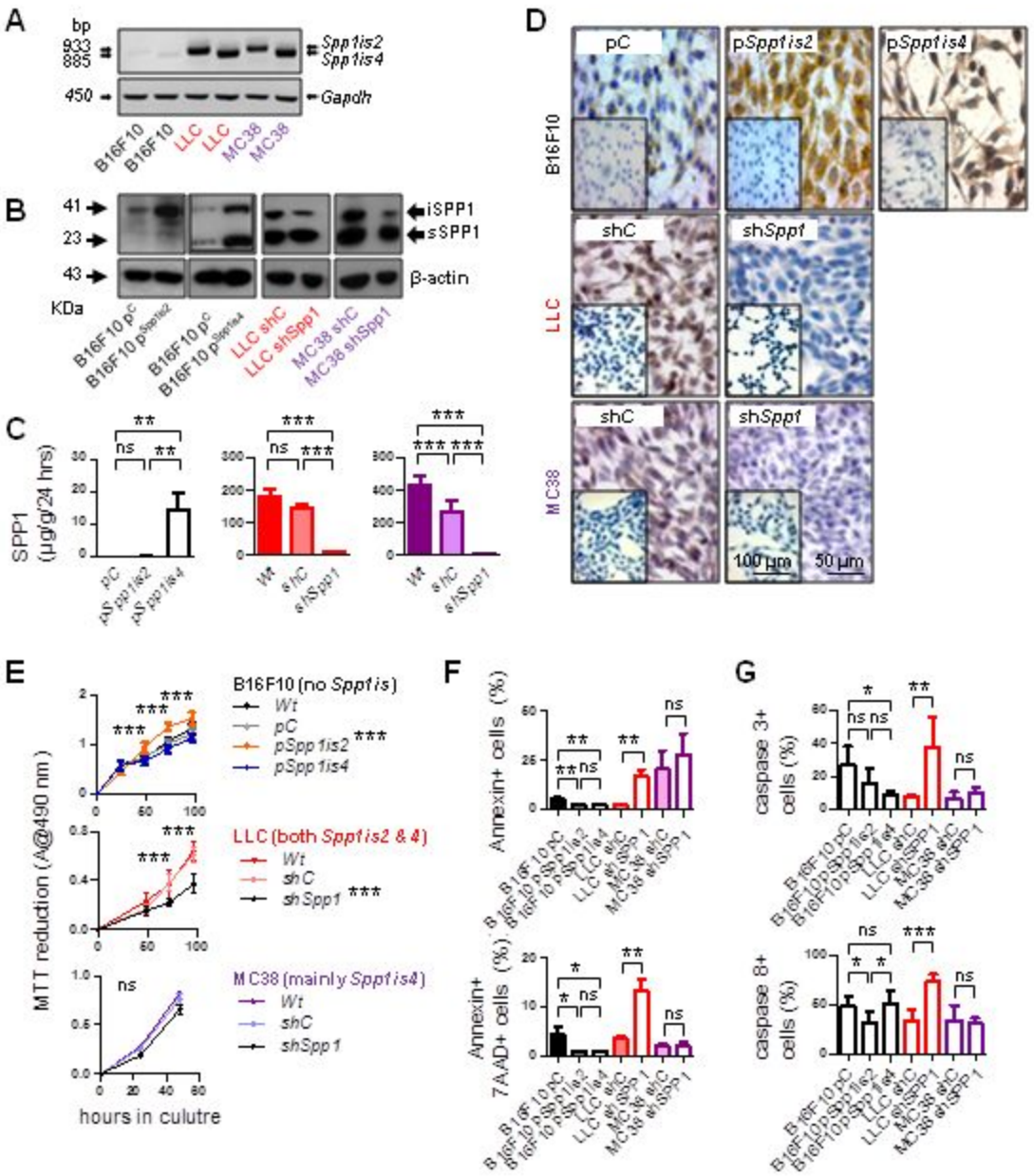
A
bp
933
885
Spp1is2
Spp1is4
450
Gapdh
B16F10
B16F10
LLC
LLC
MC38
MC38
B
41
23
43
iSPP1
sSPP1
β-actin
KDa
B16F10 pC
B16F10 pSpp1is2
B16F10 pC
B16F10 pSpp1is4
LLC shC
LLC shSpp1
MC38 shC
MC38 shSpp1
C
SPP1 (µg/g/24 hrs)
pC
pSpp1is2
pSpp1is4
Wt
shC
shSpp1
D
pC
pSpp1is2
pSpp1is4
B16F10
shC
shSpp1
LLC
shC
shSpp1
MC38
100 µm
50 µm
E
MTT reduction (A@490 nm)
hours in culutre
B16F10 (no Spp1is)
Wt
pC
pSpp1is2
pSpp1is4
LLC (both Spp1is2 & 4)
Wt
shC
shSpp1
MC38 (mainly Spp1is4)
Wt
shC
shSpp1
F
Annexin+ cells (%)
Annexin+ 7AAD+ cells (%)
G
caspase 3+ cells (%)
caspase 8+ cells (%)

Figure 3

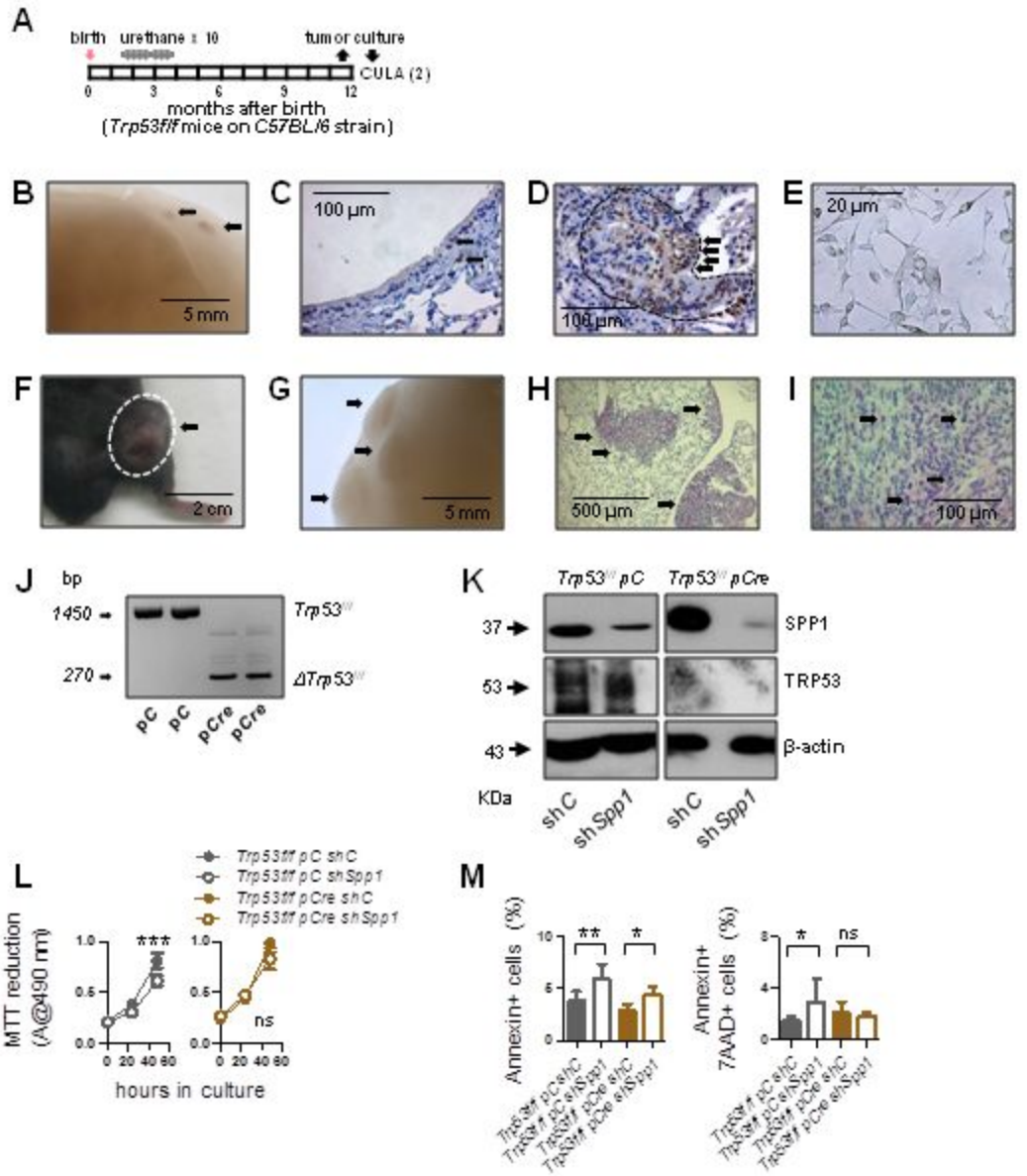
A
birth
urethane ± 10
tumor culture
CULA (2)
0
3
6
9
12
months after birth
(Trp53f/f mice on C57BL/6 strain)
B
5 mm
C
100 µm
D
100 µm
E
20 µm
F
2 cm
G
5 mm
H
500 µm
I
100 µm
J
bp
1450
270
Trp53f/f
ΔTrp53f/f
pC
pC
pCre
pCre
K
Trp53f/f pC
Trp53f/f pCre
37
53
43
SPP1
TRP53
β-actin
KDa
shC
shSpp1
shC
shSpp1
L
Trp53f/f pC shC
Trp53f/f pC shSpp1
Trp53f/f pCre shC
Trp53f/f pCre shSpp1
MTT reduction
(A@490 nm)
***
ns
hours in culture
M
Annexin+ cells (%)
**
*
Annexin+
7AAD+ cells (%)
*
ns
Trp53f/f pC shC
Trp53f/f pC shSpp1
Trp53f/f pCre shC
Trp53f/f pCre shSpp1

Figure 4

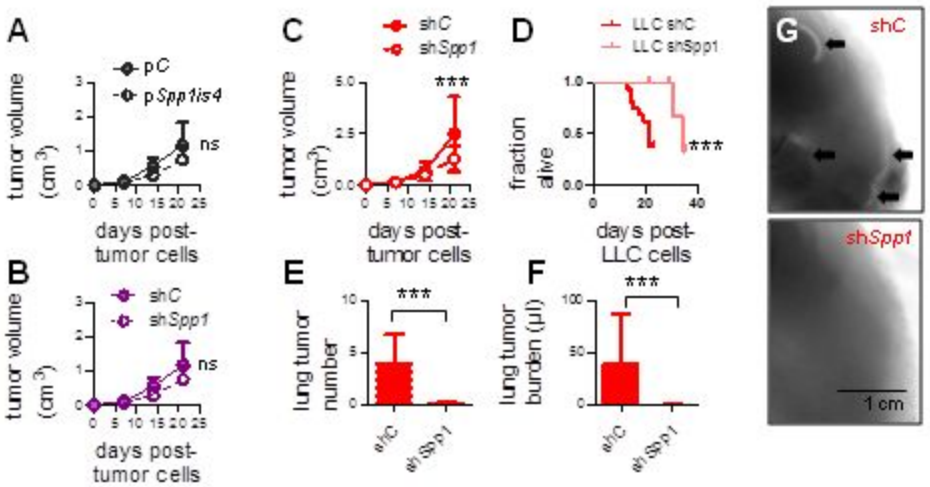
A
pC
pSpp1is4
tumor volume (cm3)
ns
days post-tumor cells
B
shC
shSpp1
tumor volume (cm3)
ns
days post-tumor cells
C
shC
shSpp1
tumor volume (cm3)
***
days post-tumor cells
D
LLC shC
LLC shSpp1
fraction alive
***
days post-LLC cells
E
***
lung tumor number
shC
shSpp1
F
***
lung tumor burden (µl)
shC
shSpp1
G
shC
shSpp1
1 cm

Figure 5

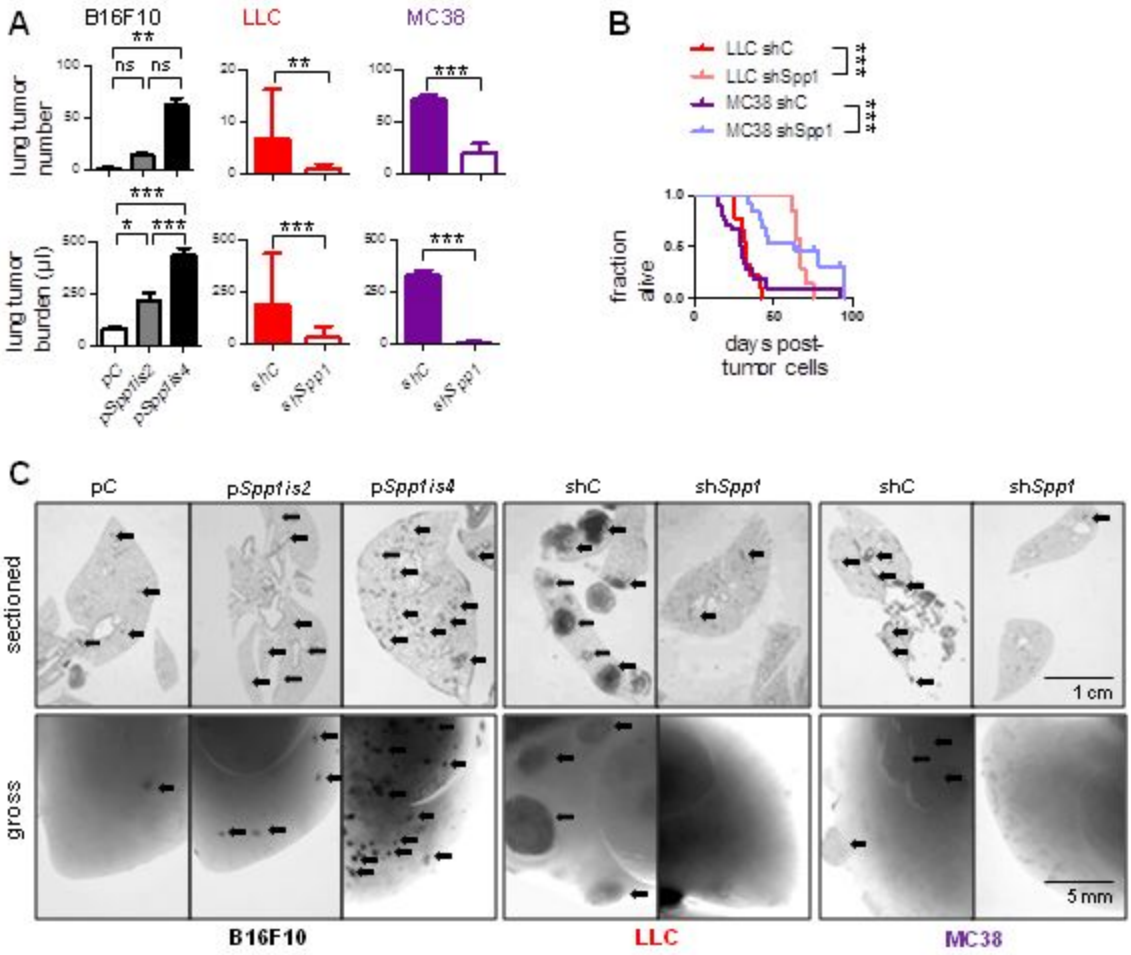
A
B16F10
LLC
MC38
lung tumor number
lung tumor burden (µl)
ns
**
***
*
pC
pSppt1is2
pSppt1is4
shC
shSpp1
B
LLC shC
LLC shSpp1
MC38 shC
MC38 shSpp1
fraction alive
days post-tumor cells
C
pC
pSppt1is2
pSppt1is4
shC
shSppt1
sectioned
gross
1 cm
5 mm
B16F10
LLC
MC38

Figure 6

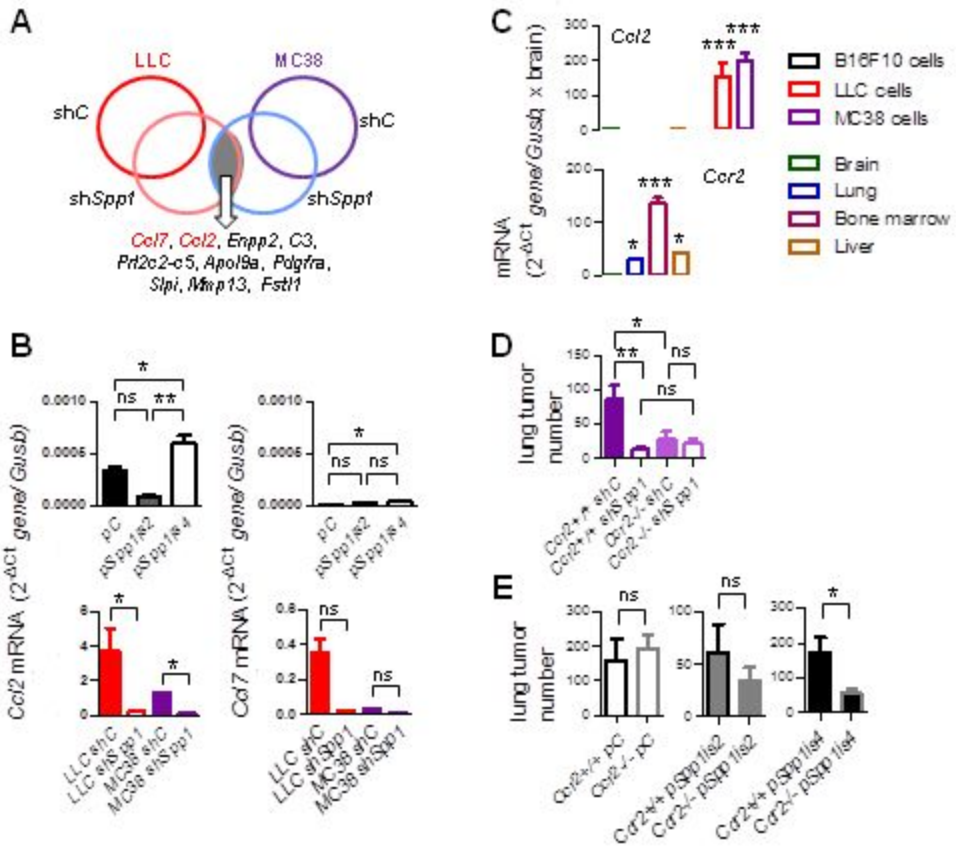
A
LLC
MC38
shC
shC
shSpp1
shSpp1
Ccl7, Ccl2, Enpp2, C3,
Prl2c2-c5, Apol9a, Pdgfra,
Slpi, Mmp13, Fstl1
B
Ccl2 mRNA (2^ΔCt gene/Gusb)
Ccl7 mRNA (2^ΔCt gene/Gusb)
pC
pSpp1#2
pSpp1#4
LLC shC
LLC shSpp1
MC38 shC
MC38 shSpp1
C
mRNA (2^ΔCt gene/Gusb x brain)
Ccl2
Ccr2
B16F10 cells
LLC cells
MC38 cells
Brain
Lung
Bone marrow
Liver
D
lung tumor number
Ccr2+/+ shC
Ccr2+/+ shSpp1
Ccr2-/- shC
Ccr2-/- shSpp1
E
lung tumor number
Ccr2+/+ pC
Ccr2-/- pC
Ccr2+/+ pSpp1#2
Ccr2-/- pSpp1#2
Ccr2+/+ pSpp1#4
Ccr2-/- pSpp1#4